NJC

Accepted Manuscript

This is an *Accepted Manuscript*, which has been through the Royal Society of Chemistry peer review process and has been accepted for publication.

Accepted Manuscripts are published online shortly after acceptance, before technical editing, formatting and proof reading. Using this free service, authors can make their results available to the community, in citable form, before we publish the edited article. We will replace this *Accepted Manuscript* with the edited and formatted *Advance Article* as soon as it is available.

You can find more information about *Accepted Manuscripts* in the Information for Authors.

Please note that technical editing may introduce minor changes to the text and/or graphics, which may alter content. The journal's standard Terms & Conditions and the Ethical guidelines still apply. In no event shall the Royal Society of Chemistry be held responsible for any errors or omissions in this *Accepted Manuscript* or any consequences arising from the use of any information it contains.

ROYAL SOCIETY OF CHEMISTRY

www.rsc.org/njc

Journal Name

RSCPublishing

ARTICLE

Template controlled synthesis of cluster-based porous coordination polymer : crystal structure, magnetism and adsorption

Cite this: DOI: 10.1039/x0xx00000x

Received 00th January 2012,
Accepted 00th January 2012

DOI: 10.1039/x0xx00000x

www.rsc.org/

Xi Chen,[a] Zhao Li,[a] Rong-jia Wei,[b] Bao Li, *,[a] Tian-le Zhang, *,[a] Jun Tao[b]

Abstract: Two distinct template mediated coordination polymers $[Co_3(ina)_4(N_3)_2(CH_3OH)_2]$ with tri-nuclear nodes (1), and $[Co_8(OH)(ina)_8(N_3)_8•X]$ with dual tetra-nuclear cobalt nodes (2) have been synthesized under hydrothermal conditions by utilizing the template agent of pentaerythritol. 1 shows 2D layer comprised of linear tri-nuclear Co^{II} clusters, in which the central cobalt ion is inter-linked with two terminal ones via mixed bridges as syn-syn carboxylate and end-on azide ion. In contrast, compound 2 exhibits a three-dimensional framework based on two kinds of six-connected tetra-nuclear cobalt clusters: square-planar node and cuboidal node. Both 1 and 2 might exhibit spin-canted magnetism. In addition, the activated sample of 2 exhibits the sorption ability of H_2 and CO_2 molecules.

Introduction

The rational construction of cluster-based porous coordination polymers (PCPs) has attracted great attention in recent years, and progress has been made in the aspects of stability, porosity and pore size/shape, which are considered as the essential ingredients of applications as storage, separation and catalysis.[1-6] The utilization of metal clusters as secondary building blocks (SBUs) has proved to be a feasible method to construct unusual PCPs with one or more desirable properties. However, despite such superiorities of cluster-based PCPs, the rational construction of PCPs is still unconsummated due to not only the difficulty in predicting the specific metal-organic connectivity and the coordination geometry of metal centers, but the variable factors that affect the self-assembly process of PCPs.[2-6] Usually, due to the naturally self-assemble process of crystallization, homogeneous type of metallic cluster acted as the nodes are stabilized in PCPs. In contrast, two or more types of different clusters consisted in one PCP is rarely presented.[7-8] Recent studies have also shown that the introduction of proper template would be of one effective way to modulate novel network topologies with anticipated properties.[9] Template species, also called structure-directing agents, is an isolated entity in the PCP frameworks, but play an important role in directing the self-assembly of the extended frameworks. The commonly used templates include solvent molecules, tetraalkylammonium cations, counter anions and additional phenyl derivatives.[10-11]The template of organic alcohols had been widely used in the synthesis process of nanomaterials. In contrast, polyhydroxyl organic molecules acted as templates for PCPs had received less academic attention.

In addition, pyridyl-carboxylates have been also confirmed as proper ligands to construct cluster-based PCPs because of their multi-directional and variable coordinated characteristic.[12-13] Therefore, the combination of pyridyl-carboxylates and proper template guests would be facile to build novel cluster-based PCPs with anticipated functional properties. With all the above considerations in mind, the simplest pyridyl-carboxylates, isonicotinic acid (Hina), and pentaerythritol acted as the template molecule are selected to construct cluster-based PCPs with cobalt ion and azide. Herein, we reported two distinct template mediated CPs, $[Co_3(ina)_4(N_3)_2(CH_3OH)_2]$ with tri-nuclear nodes (**1**), and $[Co_8(OH)(ina)_8(N_3)_8•X]$ with dual tetra-nuclear cobalt nodes (**2**). In addition, the variable temperature magnetic properties and adsorption properties have been investigated and described as follows.

Results and discussion

Synthesis of 1 and 2

The crystalline compounds were synthesized from the solvothermal reactions of cobalt salts, NaN_3 and Hina in the mixed solvent of methanol and water, and their crystal data

were listed in Table 1. For the observation of template effect, only for **2**, template agent pentaerythritol, was added in the reaction solvent. In this way, two CPs with different cobalt clusters were obtained. In the IR spectrum, the characteristic absorption peaks of the azide group and other functional ones were clearly presented. The strong absorption bands around 2070 and 1350 cm^{-1} are assigned to the asymmetric or symmetric azide vibration. The strong bands in the regions of 1610-1350 cm^{-1} are assignable to the pyridine and carboxylate groups.

Table 1 crystal data of 1 and 2

Chemical formula	$C_{26}H_{24}Co_3N_{10}O_{10}$	$C_{48}H_{33}Co_8N_{32}O_{17}$
Formula Mass	813.34	1801.5
Crystal system	Monoclinic	Tetragonal
a/Å	9.2691(12)	17.4654(18)
b/Å	9.3354(13)	17.4654(18)
c/Å	18.669(3)	19.854(3)
β/°	98.925(12)	90.00
Unit cell volume/Å3	1595.9(4)	6056.3(13)
Space group	*P*2(1)/n	$I\bar{4}m2$
Z	2	2
Rint	0.0685	0.0660
Final R1 (I > 2σ(I))	0.0504	0.0994
Final R1 values (all data)	0.0699	0.1136

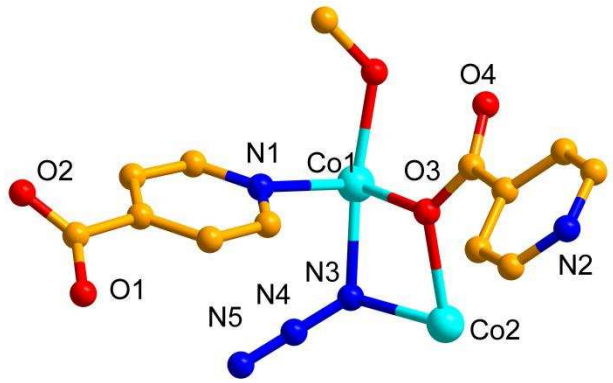

Figure 1. The perspective view of the asymmetric structure of 1 (30% probability) along with the atom numbering scheme (H atoms were omitted for clarity).

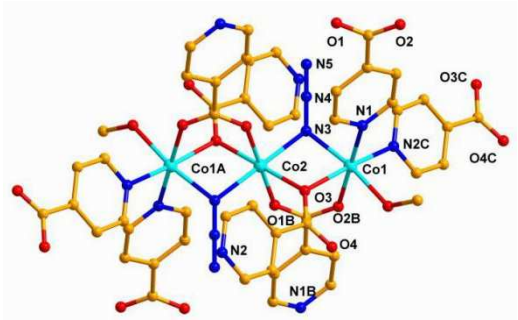

Figure 2. The perspective view of the cobalt coordination environments showing the mixed-bridges of carboxylate and azide in the trimer of 1. All hydrogen atoms are omitted for clarity.

Crystal structure of 1

The X-ray single crystal diffraction study indicates that **1** crystallizes in the monoclinic crystal system *P*2(1)/*n*, and a 2D layer crystal structure with tri-nuclear cobalt centers is presented. The asymmetric unit contains one and half cobalt ions, one coordinated methanol molecule, one independent end-on azide ion and two independent ina ligands (Figure 1). From the core structure it can be seen that the Co1 and Co2 centers are nonequivalent in terms of their coordination environments. The Co1 center is coordinated by three oxygen atoms from two different carboxylates of ina ligands (O2 from *syn-syn* carboxylate, and μ_2-bridged O3 atom) and one methanol molecule, and three nitrogen atom from two ina ligands and one end-on azide ion (Co1-O = 2.080(2) and 2.221(1) Å; Co1-N = 2.088(1) and 2.173(2) Å); the Co2 centre is bound to four ina ligands through four oxygen atoms of carboxylates and two azide ions (Co2-O = 2.039(2) and 2.203(1) Å; Co2-N = 2.113(2) Å). All of these values are in consistent with the reported Co(II) systems.[14] The central Co2 atom lies on a crystallographic inversion center and is linked by end-on azide anion and *syn-syn* carboxylate to the terminal Co1 atoms. In this way, linear tri-nuclear cobalt unit is formed and stabilized by eight coordinated ina ligands (Figure 2). Linear Co(II) trimers have been reported by several groups, normally bridged by dipyridylamine and carboxylate ligands.[14-15] To our knowledge, the linear Co(II) trimers with mixed carboxylate and azide bridging ligands are rarely reported. The distance between the neighboring Co(II) atoms is 3.21 Å, similar to other Co(II) trimers.[15] In structure of **1**, each trimer is further inter-linked by the coordinated ina ligands to result in 2D layer structure, shown in figure 3. No obvious π-π interactions could be observed in the 2D layer. Considering the trimers and ina ligands as four- and two-connecting nodes, the 2D sheet of **1** topologically possesses a 4-connected uninodal *sql*/Shubnikov tetragonal plane net with the point (Schläfli) symbol $\{4^4 \bullet 6^2\}$ calculated with TOPOS software.[16] Thus interleaved sql/Shubnikov tetragonal plane net stack over each other along *c* axis direction. Interestingly, a [4] tiling structure with plane net signature of $[121]_4[4\bullet4\bullet4\bullet4]$ is further presented, which not only tend to decrease the pore volume, but stabilize the whole crystal structure through weak interactions.

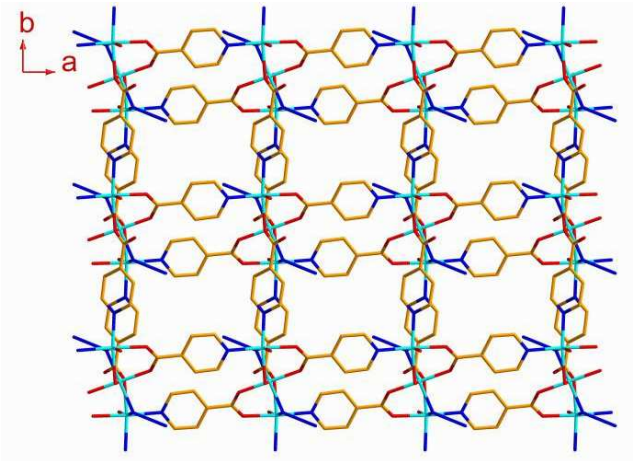

Figure 3. Partial perspective of the 2D-layer crystal structure of 1 along the crystallographic c-axis direction.

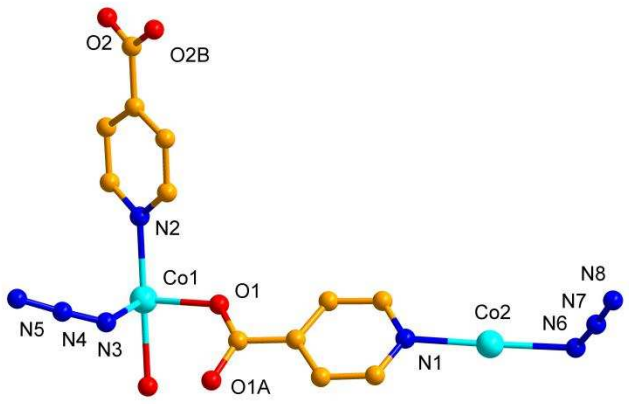

Figure 4. The perspective view of the asymmetric structure of 2 (30% probability) along with the atom numbering scheme (H atoms were omitted for clarity). Symmetric code: A, -x, y, z ; B, x, y, -z.

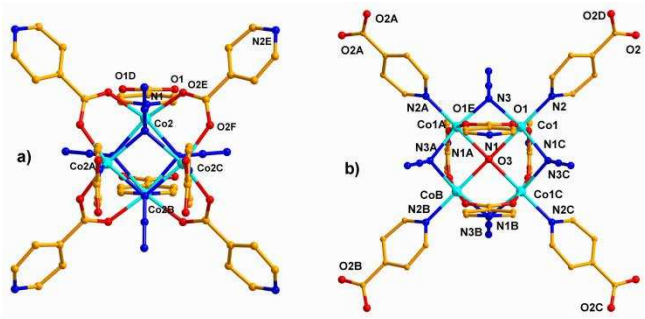

Figure 5. Perspective view of coordination modes of the cubic-Co4(a) and planar-Co4 (b) cluster-based SBUs in 2. Symmetric code:a) A, x, -y, -z+1; B, -x, -y, z; C, -x, y, -z+1; D, -x, y, z; E, -x+1/2, -y+1/2, z+1/2; F, -x+1/2, -y+1/2, -z+1/2. b) A, x, -y, -z; B, -x, -y, z; C, -x, y, -z; D, x, y, -z; E, -x, y, z.

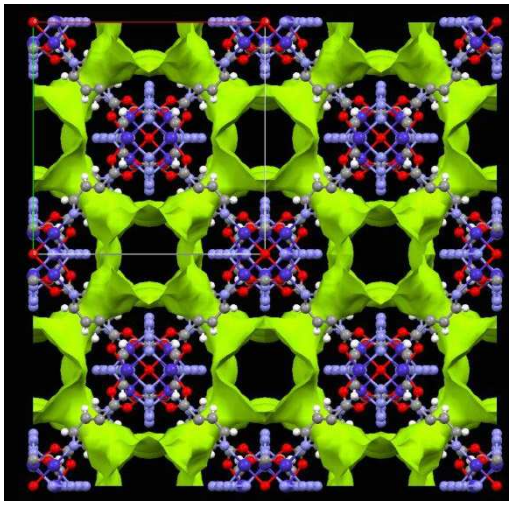

Figure 6. Partial perspective of the 3D crystal structure with 1D channels in 2 along the crystallographic c-axis direction. Green area represents the surface of coordination polymer.

Crystal structure of 2

Comparably, by adding the template agent, the novel PCP was obtained. The X-ray single crystal diffraction study indicates that **2** crystallizes in the tetragonal crystal system $I\bar{4}m2$, and an anionic 3D crystal structure with dual tetra-nuclear cobalt centers is presented. The asymmetric unit contains two half cobalt ions, one quarter oxygen atom, two half azide ions and two half ina ligands (Figure 4). From the 3D structure it can be seen that the Co1 and Co2 centers are nonequivalent and form the planar teternuclear node and cuboidal one, respectively.

The Co1 center is coordinated by three oxygen atoms from two different carboxylates of ina ligands (two O1 atoms from different *syn-syn* carboxylates, and μ_4-bridged O3 atom), and three nitrogen atom from one ina ligand and two end-on azide ions. The Co1-O bond lengths range from 2.069(2) to 2.201(1) Å, and Co1-N distances are 2.107(1) and 2.114(2) Å, corresponding the typical Co(II) state. Four edge-sharing CoO_3N_3 octahedra form a square-planar Co_4 cluster (Figure 5b). Each cobalt ion is inter-linked to the adjacent ones via end-on azide ions, *syn-syn* carboxylate of ina ligands and the μ_4-bridged O3 atom with the shortest distance of 3.11 Å. The μ_4-bridged O3 atom located in the center of tetranuclear square should be anionic OH^-.[17] In addition, each vertexes of the square is further capped by one ina ligand. In this way, a square-planar Co_4 cluster core is stabilized. Thus $[Co_4(OH)]$ cluster is very unusual because the common $[M_4(OH)]$ node reported is generally non-planar. To our knowledge, the azide-bridged square-planar $[Co_4(OH)]$ cluster had never been reported, and this is the first example observed in crystal structure.

In contrast, the Co2 center is bound to three ina ligands through two oxygen atoms of *syn-syn* carboxylates and one pyridyl N atom, three μ_3-bridged azide ions amd (Co2-O = 2.032(2) Å; Co2-N = 2.111(2) and 2.191 Å). These values are also in consistent with the typical Co(II) state. Four plane-sharing CoO_2N_4 octahedra alternating with four triply bridged azide ions at the eight corners of a cube generate a cubane core (Figure 5a). The adjacent cobalt ions were bridged by two end-on azide ions and one *syn-syn* carboxylate of ina ligands with the shortest distance of 3.11 Å. To furnish a complete octahedral coordination environment, each cobalt ion is also capped by one ina ligand. The overall arrangement has idealized D_{2d} symmetry, which has been seen in other tetra-nuclear clusters. The cuboidal core is distorted, with all the N-Co-N angles being smaller than 90°, while all the Co-N-Co angles are larger than 90°.

Each tetra-nuclear node is further cross-linked to six other sorts via the peripheral ina ligands to form the likely-NaCl lattice. In this way 1D channel with the approximate diameter of 0.5 nm along the axial c-direction were left in the structure, which are occupied by guest molecules and counter cations that could not be located via X-Ray study, shown in Figure 6. The template agent was also located even by X-Ray study and IR spectra (Figure S6). Although the pentaerythritol was not including in the final structure, it might affect the coordination environment of cobalt ions, be favor to assemble the tetra-nuclear clusters and sustain the formation of porous structure. No obvious π-π interactions could be observed in the 3D structure. Considering each tetra-nuclear units and ina ligands as four- and two-connecting nodes, the 3D structure of **2** topologically possesses a 6-connected uninodal primitive cubic with the point (Schläfli) symbol $\{4^{12}\bullet6^3\}$ calculated with TOPOS software.[16]

Thermal Stability of 1 and 2

The thermogravimetric (TG) analysis was performed in N_2 atmosphere on polycrystalline samples of complexes **1** and **2**

and the TG curves are shown in Figure S1. The TG curve of **1** show no weight loss in the temperature range of 25-200 °C, which indicates the framework retains. Along with the temperature increasing, the curve begins to drop, indicating the loss of organic ligands. For **2**, the weight loss attributed to the gradual release of three water molecules per formula unit is observed in the range of 25–120 °C (obsd: 4.38 %), then the framework retains in the temperature range of 70–250 °C, and then decompose.

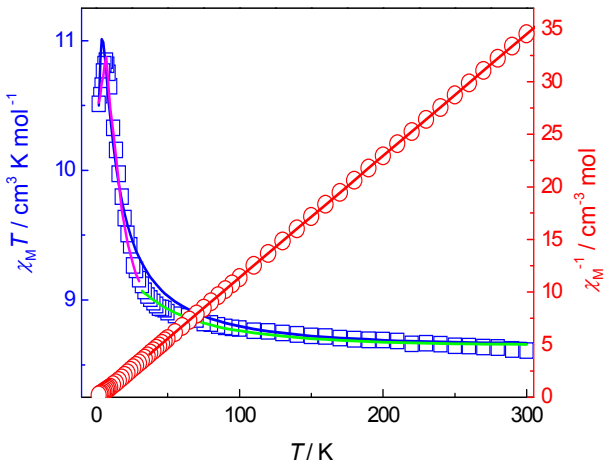

Figure 7. χ_MT and χ_M^{-1}versus T plots of 1 in the temperature range of 2-300 K under 1 kOe. The solid lines are the best fit using the Equation 1 (blue), the best fit with Seff(Co) = 1/2 at temperature below 30 K (purple) and the best fit with Si(Co) = 3/2 above 30 K (green).

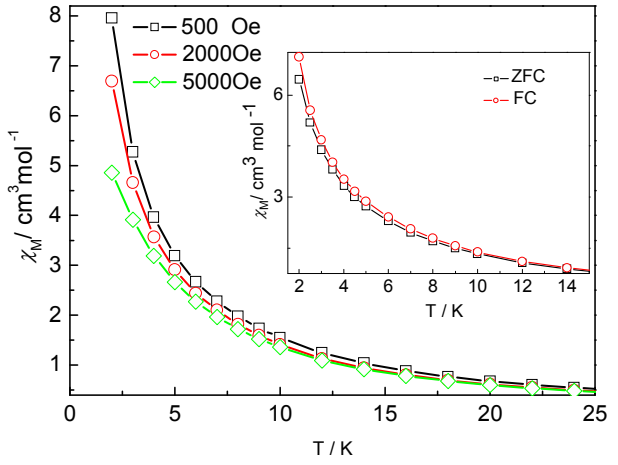

Figure 8. the field-dependent magnetic susceptibilities of 1 below 25 K. Inset: ZFCM/FCM plots for 1 at low temperature.

Magnetic studies of 1 and 2

The temperature-dependent magnetic susceptibilities for microcrystalline **1** and **2** were measured in the temperature range 2-300 K with an applied field of 1000 Oe. As shown in Fig. 7, the χ_MT value per trimer at room temperature is 8.92 cm^3 K mol^{-1}, which is large than that for three noninteracting cobalt ions of S = 3/2 because of the orbital contribution. Upon cooling, this value steadily increases to 10.88 cm^3 K mol^{-1} at 7 K, followed by a rapid decrease to 10.55 cm^3 K mol^{-1} at 2 K. The $1/\chi_M$ value above 30 K fitted with the Curie-Weiss law gave C = 8.63 cm^3 K mol^{-1} and θ = 2.04 K, which shows an intramolecular ferromagnetic coupling of the adjacent cobalt atoms.

Usually, the magnetic fitting of Co(II) systems is difficult due to the large anisotropy caused by *spin-orbital* coupling. Therefore, the following considerations by considering J and g as isotropic are quite rough. In order to simulate the experimental magnetic data, the modified Lines's model[15d] and the linear trinuclear model[15b] with two different g tensors had been adopted to fit the experimental data. However, no reasonable results could be given. Therefore, we tried to analyze the magnetic susceptibility by the corresponding expression derived through the spin Hamiltonian including the effect of the intermolecular exchange interaction (zJ') and the zero-field splitting parameter (D) in the molecular-field approximation:[18]

$$\hat{H} = -2J(\hat{S}_1 \cdot \hat{S}_2 + \hat{S}_{1A} \cdot \hat{S}_2) + D\hat{S}^2/3 \quad \text{and} \quad \chi = \frac{\chi_{trimer}}{1 - \frac{2zJ'}{Ng^2\beta^2}\chi_{trimer}} \qquad (1)$$

Where $S_1 = S_{1A} = S_2 = 3/2$. The best fit for the temperatures greater than 5 K gives g = 2.52, J = 3.28 cm^{-1}, D = 4.91 cm^{-1} and zJ' = -0.022 cm^{-1}, the calculated fit is however slightly off at temperature greater than 20 K. On the other hand, the Co(II) ion is usually treated as an effective spin $S_{Co'}$ = 1/2 at low temperature[19], thus a symmetric trimer model through Kambe's method may be used with $S_1' = S_{1A}' = S_2' = 1/2$. Fitting of the magnetic susceptibility data in the temperature range of 2-30 K gives g = 5.11, J = 6.23 cm^{-1}, and zJ' = - 0.19 cm^{-1}. Using the same method to fit the data above 30 K with S1 = S1A = S2 = 3/2 gives g = 2.54, J = 0.35 cm^{-1}, and zJ' = -0.37 cm^{-1}. All fittings give positive J values that exclusively indicate ferromagnetic coupling within the trimer.

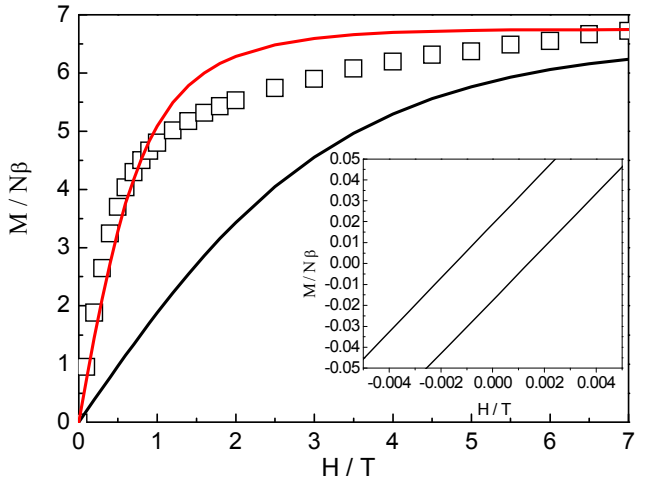

Figure 9. field dependence of the magnetization for 1 (Inset: partial view of hystersis plot). The continuous black line corresponds to the Brillouin function for three uncoupled Co^{II} ions, S = 3/2 with g=2.0, and red line represents the Brillouin function for S = 3/2 state.

To elucidate the actual coupling nature, more-detailed measurements for **1** were performed. It is noticeable that the magnetic susceptibility shows slight field dependence below 13 K, shown in Figure 8. By applying different magnetic fields, the magnetic susceptibility increases with decreasing magnetic field for **1**. Moreover, in order to characterize the low-temperature behaviors, the field-cooled (FC) and zero-field-

cooled (ZFC) magnetizations were measured at 200 Oe upon warming from 2 K to 30 K (Figure 8:inset). The ZFC and FC plots completely diverge below 12 K, suggesting the possible onset of long-range ordering or spin canting. The temperature dependencies of ac magnetic susceptibility under H_{dc}=0 Oe and H_{ac}= 3Oe had also been measured with frequencies of **1** and 1488 Hz from 2 to 20 K, no significant in-phase and out-phase ac signal signals could be detected.

The field-dependent magnetization of **1** shows a rapid increase at low fields, and almost reaches saturation at 2T (Figure 9). The magnetization at 70 kOe is 6.5 Nβ. The saturation magnetization at 70 kOe approximates to 2.15 Nβ per cobalt, which is close to the expected value gS for g=4.3 and S=1/2. The experimental magnetization is clearly above the calculated value for a sum of the Brillouin functions of three uncoupled Co centers, S = 3/2, and slightly below Brillouin function for an S = 3/2 state which might be caused by the incomplete population of the S=3/2 ground state.[20] However, the ferromagnetic interaction of Co3 cluster was confirmed. Therefore, it is reasonable to conclude that the moments of intratrimer Co atoms are aligned antiparallel. A very small hysteresis loop is observed clearly at 2.0 K giving a coercive field of $H_c \approx 18$ Oe and a remnant magnetization of M_r= 0.018 Nβ. (Figure 9: inset, S4). The canting angle can then be estimated to be about 0.16 based on the equation[13] = $\tan^{-1}$ (M_r/M_s).

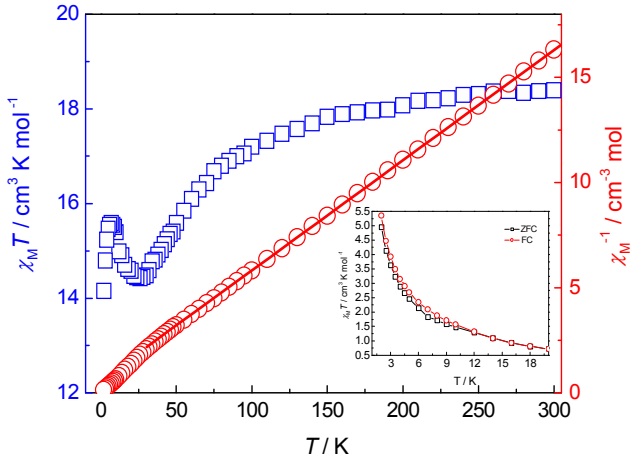

Figure 10. χ_MT and χ_M versus T plots of 2 in the temperature range of 2-300 K under 1 kOe. Inset: ZFCM/FCM plots for 2 at low temperature.

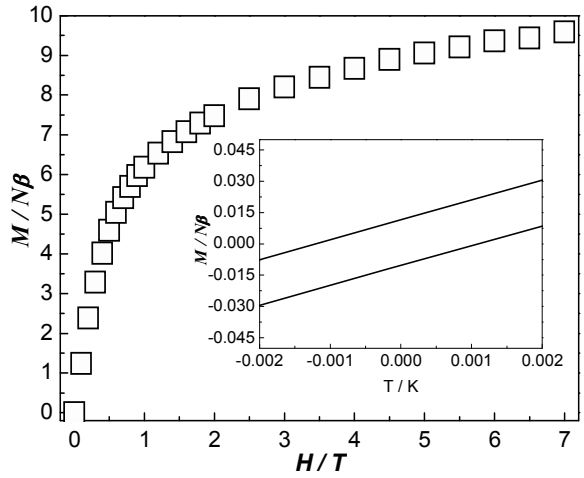

Figure 11. field dependence of the magnetization for **2** (Inset: partial view of hystersis plot.)

The χ_MT value of **2** at 300 K is about 18.15 cm^3 K mol^{-1}, higher than the experimental value of the spin-only value (15 cm^3 K mol^{-1}) expected for eight magnetically isolated high-spin d^7 Co^{II} ions, which might be caused by the unquenched orbital contributions for octahedral Co(II) ions or magnetic interactions between Co(II) ions. As the temperature is lowered, the χ_MT value decreases continuously down to 14.55 cm^3 K mol^{-1} at 24 K. Then the χ_MT value increases rapidly up to a maximum value of 15.69 cm^3 K mol^{-1} at 8 K. Upon a further decrease of the temperature lower than 8 K, the χ_MT value drops rapidly to 14.11 cm^3 K mol^{-1} at 2K because of the saturation effect. The data above 30 K follow the Curie-Weiss law with C = 19.10 cm^3 K mol^{-1} and θ = -11.19 K. In planar clusters, each cobalt ion should present antiferromagnetic interaction with adjacent one. However, in cuboidal cluster, each cobalt ion express antiferromagnetic coupling via *syn-syn* carboxyl bridges and ferromagnetic interaction by μ_3-bridged azides.

In addition, the magnetic susceptibilities of **2** shows a very slight field-dependent behavior. Moreover, a slight diverge below 12 K could be observed in the ZFC and FC plots (Figure 10:inset), suggesting the possibility of long-range ordering or spin canting. The temperature dependencies of ac magnetic susceptibility under H_{dc}=0 Oe and H_{ac}= 3Oe had also been measured with frequencies of 1 and 1488 Hz from 2 to 20 K, no significant in-phase and out-phase ac signal signals could be detected.

The field-dependent magnetization of **2** shows a gradual increase at low filed (Figure 11). At 70 kOe, the magnetization is not saturated and reaches 9.5 Nβ, lower than the expected value gS for g=4.3 and S=1/2, which might be caused by the strong antiferromagnetic coupling between cobalt ions in **2**. A very small hysteresis loop is observed clearly at 2.0 K giving a coercive field of $H_c \approx 15$ Oe and a remnant magnetization of M_r= 0.015 Nβ. (Figure 11: inset, S5). The canting angle can then be estimated to be about 0.15 based on the equation = $\tan^{-1}$ (M_r/M_s).

Gas sorption properties

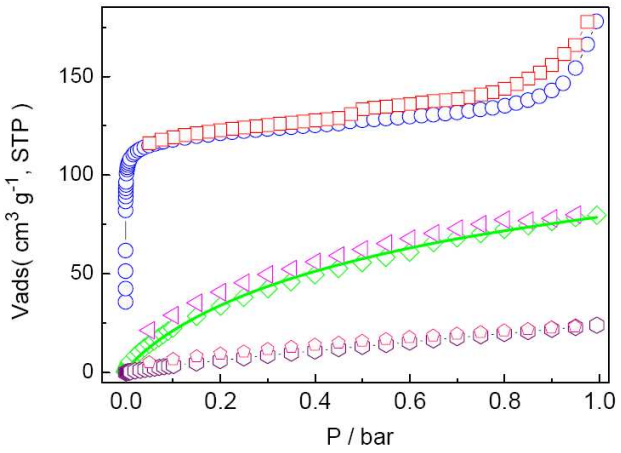

Figure 12. The sorption isotherms of N_2, H_2 and CO_2 of **2**. Blue circle, N_2 adsorption; Red square, N_2 adsorption; Green diamond, H2 adsorption; Green line, fitting of the H_2 adsorption; Purple triangle, H_2 adsorption; Pink pentagon, CO_2 adsorption; Dark-purple hexagon, CO_2 adsorption.

The highly porous and stable framework makes **2** a good candidate for gas storage. To check the permanent porosities of **2**, N_2 sorption isotherms at 77 K were collected for the desolvated samples obtained by soaking **2** in MeOH and acetone and then vacuum-drying at room temperature and at 120 °C overnight, respectively. The color of sample changes from light-red to dark-red, indicating the loss of guest molecules. As shown in Figure 12, **2** displays typical Type-I adsorption isotherms with a small hystersis, corresponding to the other ones of micro-porous materials. As expected, Sample **2** adsorbs 155 cm^3/g of N_2 at 77 K, and the Brunauer-Emmett-Teller (BET) and Langmuir surface areas are 482 m^2/g and 738 m^2/g, respectively, similar to other reported PCPs constructed by cobalt ions and ina ligand. This phenomenon encourages us to explore their potential capabilities on H_2 storage and CO_2 adsorption.

Low-pressure H_2 uptakes of desolvated samples of **2** were continuously determined using volumetric gas adsorption measurements. The adsorption isotherms also present a small hysteresis, and exhibit 80 cm^3/g (0.71 wt%) H_2 uptake under the conditions of 77K and 1 bar (Figure 12). A predicted saturation of 1.53 wt% H_2 uptake is given by a fit of the Langmuir-Freundlich equation to the H_2 uptake data.[20] This value is lower than $[Co_7(OH)_4(H_2O)_2(ina)_4(pip)_3]\cdot 10H_2O$[13c] (pip = 5-phenyl- isophthalate), which might be ascribed to the lack of effective interaction sites, such as open metal sites. In addition, the de-sorption curve confirms that 63% of the adsorbed H_2 is trapped in the framework while the pressure is reduced from 1.0 bar to 0.3 bar, and 27% of the adsorbed H_2 remains when the pressure is further reduced to 0.05 bar. Similarly, due to the lack of open metal sites and other interaction sites, the adsorption amount of CO_2 (23 cm^3/g) is also low than the other ina-based PCPs (Figure 12). The XRD pattern of bulk crystalline samples after the adsorption experiments is similar to the one simulated from the single-crystal structure and fresh samples of **2** (Figure S3), which further supported the sustained porosity and stable framework.

Conclusions

In summary, two coordination polymers with different SBUs have been synthesized under hydrothermal conditions by utilizing the template agent of pentaerythritol. **1** shows 2D layer comprised of linear trinuclear Co^{II} clusters, in which the central cobalt ion is inter-linked with two terminal ones via mixed bridges as *syn-syn* carboxylate and end-on azide ion. In contrast, compound **2** exhibits a three-dimensional framework based on two kinds of six-connected tetra-nuclear cobalt clusters: square-planar node and cuboidal node. Both **1** and **2** might exhibit spin-canted magnetism. In addition, the activated sample of **2** exhibits the sorption ability of H_2 and CO_2 molecules. This article demonstrates that the introduction of proper template agent could be a powerful way to design and explore multifunctional cluster-based PCPs featuring magnetic properties and gas storage.

Acknowledgements

We gratefully acknowledge the National Natural Science Foundation of China (no. 21471062, 21101066) and Wuhan Science and Technology Bureau (no. 201271031384) for financial support, and the Analytical and Testing Center, Huazhong University of Science and Technology for analysis and spectral measurements.

Notes and references

[a] School of Chemistry and Chemical Engineering, Huazhong University of Science and Technology, 1037 Luoyu Road, Wuhan 430074 (China). Email:libao@hust.edu.cn;tlzhang@hust.edu.cn

[b] College of Chemistry and Chemical Engineering, Xiamen University, Xiamen 361005 (China)

Electronic Supplementary Information (ESI) available:Detailed crystal data, XRD, structure figures and low-temperature heat capacity were gathered. See DOI: 10.1039/b000000x/

1 (a) L. J. Murray, M. Dinca and J. R. Long, *Chem. Soc. Rev.*, 2009, **38**, 1294-1314; (b) X. H. Bu, F. Y. Liang, Y. S. Li, J. Cravillon, M. Wiebcke and J. Caro, *J. Am. Chem. Soc.*, 2009, **131**, 16000-16001; (c) S.-G. Deng, D. Saha, Z.-B. Bao and F. Jia, *Environ. Sci. Technol.*, 2010, **44**, 1820-1826; (d) O. M. Yaghi, M. O'Keeffe, N. W. Ockwig, H. K. Chae, M. Eddaoudi and J. Kim, *Nature*, 2003, **423**, 705-714.

2 (a) J. Lee, O. K. Farha, J. Roberts, K. A. Scheidt, S. T. Nguyen and J. T. Hupp, *Chem. Soc. Rev.*, 2009, **38**, 1450-1459; (b) H.-H. Fei, D. L. Rogow and S. R. Oliver, *J. Am. Chem. Soc.*, 2010, **132**, 7202-7209; (c) F. Gándara, B. Gomez-Lor, E. Gutiérrez-Puebla, M. Iglesias, M. A. Monge, D. M. Proserpio and N. Snejko, *Chem. Mater.*, 2008, **20**, 72-76.

3 (a) G. J. Halder, C. J. Kepert, B. Moubaraki, K. S. Murray and J. D. Cashion, *Science*, 2002, **298**, 1762-1765; (b) M.-H. Zeng, M.-X. Yao, H. Liang, W.-X. Zhang and X.-M. Chen, *Angew. Chem. Int. Ed.*, 2007, **46**, 1832-1835; (c) J. Li, J. Tao, R.-B. Huang and L.-S. Zheng, *Inorg. Chem.*, 2012, **51**, 5988-5990; (d) Bao Li, Xi Chen, Fan Yu, Wenjing Yu, Tianle Zhang and Di Sun, *Cryst. Growth Des.*, 2014, **14**, 410−413.

4 (a) J.-R. Li, Y. Tao, Q. Yu and X.-H. Bu, *Chem. Commun.*, 2007, 1527-1529; (b) L. Hou, J.-P. Zhang, X.-M. Chen and S.-W. Ng, *Chem. Commun.*, 2008, 4019-4021; (c) Q.-R. Fang, G.-S. Zhu, Z. Jin, M. Xue, X. Wei, D.-J. Wang and S.-L. Qiu, *Angew. Chem. Int. Ed.*,

2006, **45**, 6126-6130; (d) B. Li, X. Dai, X. Meng, T. Zhang, C. Liu and K. Yu, *Dalton Trans.*, 2013, **42**, 2588-2593.

5 (a) U. Schubert, *Chem. Soc. Rev.*, 2011, **40**, 575-582; (b) D. J. Tranchemontagne, J. L. Mendoza-Cort_es, M. O'Keeffe and O. M. Yaghi, *Chem. Soc. Rev*., 2009, **38**, 1257-1283; (c) J. J. Perry IV, J. A. Perman and M. J. Zaworotko, *Chem. Soc. Rev.*, 2009, **38**, 1400-1417; (d) J. Li, P. Huang, X. Wu, J. Tao, R. Huang and L. Zheng. *Chem. Sci.*, 2013, **4**, 3232–3238.

6 (a)Y.. Zhang, H. Furukawa, N. Ko, W. Nie, H. J. Park, S. Okajima, K. E. Cordova, H. Deng, J. Kim, O. M. Yaghi, *J. Am. Chem. Soc.*, 2015, **137**, 2641-2650; (b) J. Zhang, X.-C. Huang and X.-M. Chen, *Chem. Soc. Rev.*, 2009, **38**, 2385-2936; (c) W. Yu, X. Chen, J. Li, B. Li, T. Zhang and J. Tao, *CrystEngComm*, 2013, **15**, 7732 – 7739.

7 (a) Y. Takashima, V. M. Martínez, S. Furukawa, M. Kondo, S. Shimomura, H. Uehara, M. Nakahama, K. Sugimoto and S.Kitagawa, *Nat. Commun.*, 2011, **2**, 168-175; (b) R. Yao, X. Xu and X. M. Zhang, *Chem. Mater.*, 2012, **24**, 303-310 ; (c) J. J. Perry, J. A. Perman and M. J. Zaworotko, *Chem. Soc. Rev.*, 2009, **38**, 1400-1417; (d) Z. Yin, Q. Wang and M. Zeng, *J. Am. Chem. Soc.*, 2012, **134**, 4857-4863; (e) Y. Bai, J. Tao, R. Huang and L. Zheng, *Angew. Chem.*, 2008, **120**, 5424-5427; *Angew. Chem. Int. Ed.*, 2008, **47**, 5344-5347.

8 (a) M. Eddaoudi, J. Kim, N. Rosi, D. Vodak, J. Wachter, M. O'Keeffe and O. M. Yaghi, *Science*, 2002, **295**, 469-472; (b) K. Koh, A. G. Wong-Foy and A. J. Matzger, *J. Am. Chem. Soc.*, 2009, **131**, 4184-4185; (c) K. S. Min and M. P. Suh, *J. Am. Chem. Soc.*, 2000, **122**, 6834-6840; (b) Q. Y. Yang, K. Li, J. Luo, M. Pana and C. Y. Su, *Chem. Commun.*, 2011, **47**, 4234-4236; (d) J. An and N. L. Rosi, *J. Am. Chem. Soc.*, 2010, **132**, 5578-5579; (e) J. Li, J. Tao, R. Huang and L. Zheng, *Inorg. Chem.*, 2012, **51**, 5988-5990.

9 (a) Q. Chen, J.-B. Lin, W. Xue, M.-H. Zeng and X.-M. Chen, *Inorg. Chem.*, 2011, **50**, 2321-2328; (b) Q. Chen, W. Xue, B.-Y. Wang, M.-H. Zeng and X.-M. Chen, *CrystEngComm*, 2012, **14**, 2009–2014.

10 (a) D. Tanaka and S. Kitagawa, *Chem Mater.*, 2008, **20**, 922–931; (b) Q. Chen, M. H. Zeng, L. Q. Wei and M. Kurmoo *Chem Mater.*, 2010, **22**, 4328–4334; (c) L. Dobrzańska, G. O. Lloyd, H. G. Raubenheimer and L. J. Barbour, *J. Am. Chem. Soc.*, 2005, **127**, 13134–13135.

11 (a) L. Ma and W. Lin, *J. Am. Chem. Soc.*, 2008, **130**, 13834–13835; (b) D. Braga, S. d'Agostino and F. Grepioni, *Cryst. Growth Des.*, 2012, **12**, 4880−4889; (c) X. Huang, J. Zhang and X. Chen, *J. Am. Chem. Soc.*, 2004, **126**, 13218-13219; (d) S. R. Halper, L. I. Do, J. R. Stork and S. M. Cohen, *J. Am. Chem. Soc.*, 2006, **128**, 15255-15268.

12 (a) F. Liu, Y. Zeng, J. Jiao, X. Bu, J. Ribas, and S. R. Batten, *Inorg. Chem.*, 2006, **45**, 2776-2778; (b) J. Zhao, B. Hu, X. Zhang, Q. Yang, M. S. El Fallah, J. Ribas and X. Bu, *Inorg. Chem.*, 2010, **49**, 11325–11332; (c) M. Zeng, Y. Zhou, M. Wu, H. Sun and M. Du, *Inorg. Chem.*, 2010, **49**, 6436–6442.

13 (a) M. Zeng, Z. Yin, Y. Tan, W. Zhang, Y. He and M. Kurmoo, *J. Am. Chem. Soc.*, 2014, **136**, 4680-4688; (b) Y. Hu, M. Zeng, K. Zhang, S. Hu, F. Zhou and M. Kurmoo, *J. Am. Chem. Soc.*, 2013, **135**, 7901-7908; (c) J. Li, B. Li, P. Huang, H. Shi, R. Huang, L. Zheng and J. Tao, *Inorg. Chem.*, 2013, **52**, 11573−11579;(d)Y. Kang and F. Wang,*CrystEngComm*, 2014,**16**, 4088-4090; (e) P. Pachfule, Y. Chen, J. Jiang and R. Banerjee, *Chem. Eur. J.* 2012, **18**, 688-694.

14 (a) F. A. Cotton, L. M. Daniels, G. T. Jordan IV and C. A. Murillo, *J. Am. Chem. Soc.*, 1997, **119**, 10377-10381; (b) R. Clérac, F. A. Cotton, K. R. Dunbar, T. Lu, C. A. Murillo and X. Wang, *Inorg. Chem.*, 2000, **39**, 3065-3070; (c) D. A. Pantazis and J. E. McGrady, *J. Am. Chem. Soc.*, 2006, **128**, 4128-4135.

15 (a) B.-H. Ye, X.-M. Chen, F. Xue, L.-N. Ji and T. C. W. Mak, *Inorg. Chim. Acta*, 2000, **299**, 1-10; (b) T. Yi, C.-H. Chol, S. Gao and S. Kitagawa, *Eur. J. Inorg. Chem.*, 2006, 1381-1387; (c) D. Mandal, M. Mikuriya, H. K. Fun and D. Ray, *Inorg. Chem. Commun.*, 2007, **10**, 657-660 ; (d) Y. Oka and K. Inoue, *Chem. Lett.*, 2004, **33**, 402-403.

16 V. A. Blatov, *Struct. Chem.*, 2012, **23**, 955-963.

17 (a) J. Zhang, R.i Liu, P. Feng and X. Bu, *Angew. Chem. Int. Ed.*, 2007, **46**, 8388-8391.(a) S. Du, C. Hu, J. Xiao, H. Tana and W. Liao, *Chem. Commun.*, 2012, **48**, 9177-9179.

18 (a) K. Kambe, *J. Phys. Soc. Jpn.*, 1950, **5**, 48-51; (b) X. Lin, J. Tao, R. Huang and L. Zheng, *Inorg. Chem. Commun.*, 2009,**12**, 154-156.

19 (a) S. Dominguez, A. Mederos, P. Gili, A. Rancel, A. E. Rivero, F. Brito, F. Lloret, X. Solans, C. Ruiz-Perez and M. L. Rodriguez, *Inorg. Chim. Acta*, 1997, **255**, 367-380; (b) J. M. Herrera, A. Bleuzen, Y. Dromzée, M. Julve, F. Lloret and M. Verdaguer, *Inorg. Chem.*, 2003, **42**, 7052-7059; (c) D. Maspoch, N. Domingo, D. Ruiz-Molina, K. Wurst, J. M. Hernández, G. Vaughan, C. Rovira, F. Lloret, J. Tejada and J. Veciana, *Chem. Commun*.,2005, 5035-5037.

20 (a)J. Boonmak, M. Nakanob and S. Youngme，*Dalton Trans.*, **2011**, *40*, 1254-1260; (b)M.l Ryazanov, S. Troyanov, M. Baran , R. Szymczak and N. Kuzmina,*Polyhedron*, **2004**, *23*, 879 – 883.